Electrical Power and Energy Systems 54 (2014) 367–375

Contents lists available at ScienceDirect

Electrical Power and Energy Systems

journal homepage: www.elsevier.com/locate/ijepes

A widely linear least mean phase algorithm for adaptive frequency estimation of unbalanced power systems

Yili Xia [a,b,*], Danilo P. Mandic [b]

[a] School of Information Science and Engineering, Southeast University, CNV A5-409, 9 Mozhoudonglu, Jiangning District, Nanjing 211111, PR China
[b] Department of Electrical and Electronic Engineering, Imperial College London, London SW7 2BT, UK

ARTICLE INFO

Article history:
Received 9 August 2012
Received in revised form 17 July 2013
Accepted 23 July 2013

Keywords:
Frequency estimation
Least mean phase
Widely linear model
Complex noncircularity
Phase-only estimation
Unbalanced three-phase power system

ABSTRACT

A robust technique for online estimation of the fundamental frequency of both balanced and unbalanced three-phase power systems is proposed. This is achieved by introducing a widely linear least mean phase (WL-LMP) frequency estimator, based on Clarke's transformation and widely linear complex domain modelling. The proposed method makes use of the full second-order information within the complex-valued system voltage, making it possible to eliminate otherwise unavoidable oscillations in frequency estimation. In this way, the WL-LMP inherits the advantages of the phase-only approach, such as its high angle estimation accuracy and immunity to voltage and harmonics variations, while accounting for the noncircularity of Clarke's voltage in unbalanced conditions. Simulations over a range of unbalanced conditions, including those caused by voltage sags and higher order harmonics, and case studies for real-world unbalanced power systems support the analysis.

1. Introduction

Frequency is a key variable in power quality control, as its fluctuations reflect the dynamic balance between power generation and load consumption [1]. The need for its accurate estimation is even more highlighted through current trends for distributed generation, which require perfect system synchrony is needed to connect microgrids and regulate islanding. In those scenarios, some fluctuating loads, such as electric arc furnaces, adjustable speed drives (ASDs), and nonlinear electric devices, are sources of harmful voltage fluctuations, higher order harmonics, amplitude and phase noise, and system frequency deviation [2].

To deal with these issues in a timely and efficient way, fast and accurate frequency estimation has attracted much research effort. A variety of linear and nonlinear architectures and the associated signal processing algorithms have been developed for this purpose, including zero crossing techniques [3,4], discrete Fourier transform (DFT) based algorithms [5,6], phase-locked loops (PLL) [7,8], complex least mean square (CLMS) adaptive filters [9,10], recursive Newton-type algorithms [11], and Kalman filters [12,13]. Among these, adaptive approaches based on the minimisation of mean square error have proved very useful, owing to their simple structure, computational efficiency and stability, and robustness in the presence of noise and harmonic distortions.

There are a number of applications where the mean square error (MSE) criterion is not the most intuitive solution, particularly when the information of interest is contained predominantly in either the amplitude or phase of a complex signal. Such is the case with frequency estimation in power systems, where the desired information is primarily in the complex phasor, therefore phase error in the estimation is more critical than the amplitude error, and hence the standard MSE based CLMS is not best equipped to deal with predominantly phase error. To that cause, the recent least mean phase (LMP) algorithm employs an optimisation criterion based on the phase error [14], and has proven beneficial in communications applications (DS-CDMA receivers), where the relevant information is in the phase of the transmitted signals rather than in the magnitude. A continuous-time version of this algorithm has recently been applied to estimate the power system frequency [15], and its superiority over the standard CLMS was justified by the fact that the instantaneous frequency estimation is derived from the well-established phase angle evolution.

Although current adaptive filtering based frequency estimation algorithms are second order optimal under normal 'balanced' power system conditions, and also in noisy environments and in the presence of high order harmonics and frequency deviations, they suffer from performance degradation under unbalanced

* Corresponding author at: School of Information Science and Engineering, Southeast University, CNV A5-409, 9 Mozhoudonglu, Jiangning District, Nanjing 211111, PR China. Tel: +86(0)2584980409.
E-mail addresses: yili.xia06@gmail.com (Y. Xia), d.mandic@ic.ac.uk (D.P. Mandic).

0142-0615/$ - see front matter © 2013 Elsevier Ltd. All rights reserved.
http://dx.doi.org/10.1016/j.ijepes.2013.07.030

voltage conditions. These occur in the case of different amplitudes of the three phase voltages, or under a voltage sag in one or two phases. Their inadequacy can be explained by the fact that current adaptive filters employ the standard linear model to carry out the phase angle estimation, thus accounting only for the 'positive sequence' (with positive frequency) in the $\alpha\beta$ transform, however, the 'negative sequence' introduced by the system imbalance results in an inevitable estimation error oscillating at twice the system frequency [16].

To eliminate the bias and steady state oscillations encountered by the LMP algorithm under unbalanced system conditions, in this work, we embark upon the analysis in [17–19] and introduce the widely linear LMP (WL-LMP) algorithm, which caters for the noncircular nature of the complex-valued system voltage under the unbalanced system conditions. This allows us to rectify the issue of phase angle bias exhibited by the strictly linear LMP algorithm in unbalanced system conditions, while for balanced systems we show that WL-LMP degenerates into the strictly linear LMP.

This paper is organised as follows. In Section 2, an overview of widely linear estimation is provided. The modelling of unbalanced three-phase power system is addressed in Section 3. In Section 4, an overview of the standard LMP frequency estimator and its suboptimality under unbalanced power systems are discussed. The widely linear model, which is second order optimal for the generality of complex-valued signals, and the proposed unbiased widely linear LMP (WL-LMP) frequency estimator are introduced in Section 5. Section 6 presents the stability analysis of WL-LMP. In Section 7, simulations over a range of unbalanced and distorted conditions, including voltage sags, higher order harmonics, and real-world unbalanced power systems are provided to illustrate the unbiasedness of the proposed WL-LMP frequency estimator and its advantages over the mean squared error based widely linear complex least mean square (WL-CLMS) frequency estimator [17]. Finally, Section 8 concludes the paper.

2. Widely linear modelling

Consider a real-valued conditional mean square error (MSE) estimator $\hat{y} = E[y|\mathbf{x}]$, which estimates the signal y in terms of another observation $\mathbf{x}$. For zero mean, jointly normal y and $\mathbf{x}$, the optimal solution is given by the linear model

$$\hat{y} = \mathbf{x}^T\mathbf{w} \tag{1}$$

where $\mathbf{w} = [w_1, \ldots, w_L]^T$ is the vector of fixed filter coefficients, $\mathbf{x} = [x_1, \ldots, x_L]^T$ the regressor vector, and $(\cdot)^T$ the vector transpose operator.

In the complex domain, since both the real and imaginary parts of complex variables are real, we have

$$\begin{aligned}\Re(\hat{y}) &= E[\Re(y)|\Re(\mathbf{x}), \Im(\mathbf{x})]\\ \Im(\hat{y}) &= E[\Im(y)|\Re(\mathbf{x}), \Im(\mathbf{x})]\end{aligned} \tag{2}$$

and $\hat{y} = E[\Re(\hat{y})|\Re(\mathbf{x}), \Im(\mathbf{x})] + \jmath E[\Im(y)|\Re(\mathbf{x}), \Im(\mathbf{x})]$, where the operators $\Re(\cdot)$ and $\Im(\cdot)$ extract respectively the real and imaginary parts of a complex variable. Upon substituting $\Re(\mathbf{x}) = (\mathbf{x} + \mathbf{x}^*)/2$ and $\Im(\mathbf{x}) = (\mathbf{x} - \mathbf{x}^*)/2\jmath$, we arrive at

$$\hat{y} = E[\Re(y)|\mathbf{x}, \mathbf{x}^*] + \jmath E[\Im(y)|\mathbf{x}, \mathbf{x}^*] = E[y|\mathbf{x}, \mathbf{x}^*] \tag{3}$$

leading to the widely linear estimator

$$\hat{y} = \mathbf{h}^T\mathbf{x} + \mathbf{g}^T\mathbf{x}^* = \mathbf{x}^T\mathbf{h} + \mathbf{x}^H\mathbf{g} \tag{4}$$

where $\mathbf{h}$ and $\mathbf{g}$ are complex-valued coefficient vectors. Such a widely linear estimator is optimal for the generality of complex signals. From (4), it is apparent that the covariance matrix $\mathbf{C_{xx}} = E[\mathbf{x}\mathbf{x}^H]$ alone does not have sufficient degrees of freedom to describe full second-order statistics [20], and in order to make use of all the available statistical information, we also need to consider the pseudo-covariance matrix $\mathbf{P_{xx}} = E[\mathbf{x}\mathbf{x}^T]$. Processes whose second-order statistics can be accurately described by only the covariance matrix, that is with $\mathbf{P_{xx}} = \mathbf{0}$, are termed second-order circular (or proper), such signals have rotation-invariant distributions $\mathcal{P}[\cdot]$ for which $\mathcal{P}[\mathbf{z}] = \mathcal{P}[\mathbf{z}e^{j\theta}]$ for $\theta \in [0, 2\pi)$. However, in order to cater for second order noncircular (or improper) signals (with rotation dependent distributions), the widely linear model in (4) should be employed, whereby the regressor vector is produced by concatenating the input vector $\mathbf{x}$ with its conjugate $\mathbf{x}^*$, to give an augmented $(2L \times 1)$-dimensional input vector $\mathbf{x}^a = [\mathbf{x}^T, \ \mathbf{x}^H]^T$, together with the augmented coefficient vector $\mathbf{w}^a = [\mathbf{h}^T, \ \mathbf{g}^T]^T$. The corresponding $(2L \times 2L)$-dimensional augmented covariance matrix then becomes

$$\mathbf{C}^a_{\mathbf{xx}} = E[\mathbf{x}^a\mathbf{x}^{aH}] = E\begin{bmatrix}\mathbf{x}\\ \mathbf{x}^*\end{bmatrix}[\mathbf{x}^H\mathbf{x}^T] = \begin{bmatrix}\mathbf{C_{xx}} & \mathbf{P_{xx}}\\ \mathbf{P}^*_{\mathbf{xx}} & \mathbf{C}^*_{\mathbf{xx}}\end{bmatrix} \tag{5}$$

and contains the full second order statistical information [21–23].

3. Unbalanced three-phase power systems

The three-phase voltages of a power system in a noise-free environment can be represented in a discrete time form as

$$\begin{aligned}v_a(k) &= V_a\cos(\omega k\Delta\mathrm{T} + \phi)\\ v_b(k) &= V_b\cos\left(\omega k\Delta\mathrm{T} + \phi - \frac{2\pi}{3}\right)\\ v_c(k) &= V_c\cos\left(\omega k\Delta\mathrm{T} + \phi + \frac{2\pi}{3}\right)\end{aligned} \tag{6}$$

where V_a, V_b, V_c are the peak values of each fundamental voltage component at time instant k, $\Delta\mathrm{T} = \frac{1}{f_s}$ is the sampling interval where f_s is the sampling frequency, ϕ is the initial phase, and $\omega = 2\pi f$ is angular frequency of the voltage signal, with f being the system frequency. For analysis purpose, the time-dependent three-phase voltage in (6) is routinely transformed by the orthogonal $\alpha\beta$ transformation matrix [24] into a zero-sequence v_0 and the direct and quadrature-axis components, v_α and v_β, as

$$\begin{bmatrix}v_0(k)\\ v_\alpha(k)\\ v_\beta(k)\end{bmatrix} = \sqrt{\frac{2}{3}}\begin{bmatrix}\frac{\sqrt{2}}{2} & \frac{\sqrt{2}}{2} & \frac{\sqrt{2}}{2}\\ 1 & -\frac{1}{2} & -\frac{1}{2}\\ 0 & \frac{\sqrt{3}}{2} & -\frac{\sqrt{3}}{2}\end{bmatrix}\begin{bmatrix}v_a(k)\\ v_b(k)\\ v_c(k)\end{bmatrix} \tag{7}$$

where the factor $\sqrt{2/3}$ ensures that the system power is invariant under this transformation. In balanced system conditions, $V_a(k)$, $V_b(k)$, $V_c(k)$ are identical, giving $v_0(k) = 0$, $v_\alpha(k) = A\cos(\omega k\Delta\mathrm{T} + \phi)$ and $v_\beta(k) = A\cos(\omega k\Delta\mathrm{T} + \phi + \frac{\pi}{2})$. The amplitude, $A = \frac{\sqrt{6}(V_a+V_b+V_c)}{6}$, is constant while $v_\alpha(k)$ and $v_\beta(k)$ represent the orthogonal coordinates of a point whose position is time variant at a rate proportional to the system frequency. In practise, normally only the v_α and v_β are used to form the complex system voltage $v(k)$ (known as Clarke's transformation [25]), given by

$$v(k) = v_\alpha(k) + \jmath v_\beta(k) = Ae^{j(\omega k+\phi)} \tag{8}$$

Fig. 2(a) illustrates that for a balanced system state, the probability density function of $v(k)$ is rotation invariant (circular), since v and $ve^{j\theta}$ have the same distribution for any real θ. Statistically, this means that $v(k)$ is second order circular (proper) and with equal powers in v_α and v_β, and thus the covariance matrix, $\mathbf{C} = E[\mathbf{v}\mathbf{v}^H]$, is sufficient to fully describe the second order statistics, while the pseudocovariance matrix, $\mathbf{P} = E[\mathbf{v}\mathbf{v}^T] = \mathbf{0}$, vanishes as discussed in Section 2. However, when the three-phase power system deviates from its nominal condition, such as when the three channel voltages exhibit different levels of dips or transients, V_a, V_b, V_c are not identical and the complex $\alpha\beta$ voltage becomes

$$v(k) = v_\alpha(k) + \jmath v_\beta(k) = \underbrace{Ae^{j(\omega k\Delta T+\phi)}}_{A(k)} + \underbrace{Be^{-j(\omega k\Delta T+\phi)}}_{B(k)} \tag{9}$$

where

$$A = \frac{\sqrt{6}(V_a + V_b + V_c)}{6}$$
$$B = \frac{\sqrt{6}(2V_a - V_b - V_c)}{12} - \jmath\frac{\sqrt{2}(V_b - V_c)}{4} \tag{10}$$

This expression emerged only recently [17–19] to jointly model both the balanced and unbalanced systems, and should be used in time-varying environments. In this way, for balanced system conditions, $V_a = V_b = V_c$ and $B = 0$, for which the standard model with a circular voltage distribution is adequate, whereas for unbalanced conditions, $B \neq 0$, causing the samples of $v(k)$ generated from (9) not to be allocated on a circle with a constant radius, and thus a rotation dependent (noncircular) distribution of $v(k)$. In this case, the pseudocovariance matrix does not vanish while the covariance matrix does not have sufficient degrees of freedom to describe full second-order statistics. Hence, standard, strictly linear, signal processing in the complex domain $\mathbb{C}$, based solely on the covariance matrix is suboptimal for unbalanced systems, and widely linear modelling based on both the covariance and pseudocovariance matrix should be used in order to make use of all the available second-order information. Some examples of circular and noncircular (*cf.* balanced and unbalanced) system voltages are given in Fig. 2.

4. Least mean phase (LMP) based frequency estimation method and its suboptimality in unbalanced system conditions

The idea behind the LMP adaptive estimation is to minimise the cost function based on mean square phase angle error, given by Ref. [15,14]

$$\mathcal{J}(k) = e^2(k) \tag{11}$$

where the phase error is calculated as

$$e(k) = \angle v(k+1) - \angle \hat{v}(k+1) \tag{12}$$

and the symbol $\angle(\cdot)$ denotes the phase angle operator. Within the standard, strictly linear, LMP, the filter output $\hat{v}(k+1)$ is estimated in a strictly linear manner as

$$\hat{v}(k+1) = v(k)w(k) \tag{13}$$

where $w(k)$ is the filter weight coefficient, and is updated in a stochastic gradient manner as [14]

$$w(k+1) = w(k) - \mu\nabla_w\mathcal{J}(k) = w(k) + \frac{\jmath\mu e(k)v^*(k)}{[v(k)w(k)]^*} \tag{14}$$

where μ is the step-size which controls the convergence speed and steady state estimation accuracy, and is set to a small constant.

Note that under balanced system conditions, based on (8) the system voltage $v(k)$ evolves as

$$v(k+1) = v(k)e^{\jmath\omega\Delta T} \tag{15}$$

Upon combining with (13), the LMP frequency estimator is derived from the filter weight coefficient $w(k)$, in order to track the evolution of the rotational term $e^{\jmath\omega\Delta T}$ in (15), that is [15]

$$\hat{f}(k) = \frac{1}{2\pi\Delta T}\tan^{-1}\left(\frac{\Im(w(k))}{\Re(w(k))}\right) \tag{16}$$

The geometric analysis in [14] verifies that the term $\frac{\jmath}{[v(k)w(k)]^*}$ within the weight update in (14) aims to correct the error in the phase of the estimated signal by rotating the estimate towards the desired signal in a perpendicular direction. This allows us to track the phase/frequency variations in the desired signal in a faster and more efficient manner than using the conventional CLMS, which is designed to minimise the mean square magnitude error.

However, in critical cases when the balanced power system deviates from its nominal condition, the expression in (8) is inadequate and the system voltage $v(k)$ is only accurately expressed by Eq. (9). Then, a direct use of the strictly linear model would lead to

$$\hat{v}(k+1) = v(k)w(k) = (Ae^{j(\omega k\Delta T+\phi)} + Be^{-j(\omega k\Delta T+\phi)})w(k) \tag{17}$$

Notice that in the steady state, $\hat{v}(k+1) \approx v(k+1)$, resulting in

$$w(k) \approx \frac{v(k+1)}{v(k)} \approx \frac{Ae^{j(\omega k\Delta T+\phi)}e^{\jmath\omega\Delta T} + Be^{-j(\omega k\Delta T+\phi)}e^{-\jmath\omega\Delta T}}{Ae^{j(\omega k\Delta T+\phi)} + Be^{-j(\omega k\Delta T+\phi)}}$$
$$\approx \frac{\frac{A}{B}e^{\jmath 2(\omega k\Delta T+\phi)}e^{\jmath\omega\Delta T} + e^{-\jmath\omega\Delta T}}{\frac{A}{B}e^{\jmath 2(\omega k\Delta T+\phi)} + 1} \approx e^{\jmath\omega\Delta T} + \frac{e^{-\jmath\omega\Delta T} - e^{\jmath\omega\Delta T}}{\frac{A}{B}e^{\jmath 2(\omega k\Delta T+\phi)} + 1} \tag{18}$$

where $\frac{A}{B}$ is an unknown but nonzero parameter, indicating that the second term on the right hand side of (18) is not negligible, and results in

$$w(k) = w\left(k + \frac{1}{2f\Delta T}\right) \tag{19}$$

showing that when the strictly linear filter is applied to unbalanced system conditions, the term $w(k)$ is oscillating at twice of the system frequency. From (16), this oscillation further propagates into the estimated frequency $\hat{f}(k)$, due to the monotonicity of $\tan^{-1}(\cdot)$.

5. The Widely Linear LMP (WL-LMP) based frequency estimation

To eliminate the inevitable oscillation in system frequency estimation encountered by the standard phase angle calculation used in the strictly linear LMP, we propose to employ the widely linear model in (4) in conjunction with the LMP cost function in order to introduce the WL-LMP algorithm. We start from a general adaptive filter, and proceed to perform voltage prediction in the context of power system frequency estimation as a particular (scalar) case.

5.1. The widely linear LMP adaptive filter

Consider the output of a widely linear adaptive filter in the form,

$$y(k) = \underbrace{\mathbf{x}^T(k)\mathbf{h}(k)}_{\text{standard update}} + \underbrace{\mathbf{x}^H(k)\mathbf{g}(k)}_{\text{conjugate update}} \tag{20}$$

where $\mathbf{h}(k)$ and $\mathbf{g}(k)$ are the $L \times 1$ weight vectors of filter coefficients for standard and conjugate parts respectively, and $\mathbf{x}(k)$ denotes the $(L \times 1)$-dimensional input vector, defined as $\mathbf{x}(k) = [x(k), x(k-1), \ldots, x(k-L+1)]^T$. The squared phase angle based cost function that we wish to minimise is given by

$$\mathcal{J}(k) = |\angle d(k) - \angle y(k)|^2 = e^2(k) \tag{21}$$

where $d(k)$ is the desired signal, and the update of both the standard and conjugate weight coefficients can be obtained by using steepest descent as

$$\mathbf{h}(k+1) = \mathbf{h}(k) - \mu\nabla_{\mathbf{h}}\mathcal{J}(k) \tag{22}$$
$$\mathbf{g}(k+1) = \mathbf{g}(k) - \mu\nabla_{\mathbf{g}}\mathcal{J}(k) \tag{23}$$

where the gradient $\nabla_{\mathbf{g}}\mathcal{J}(k)$ can be derived as

$$\nabla_{\mathbf{g}}\mathcal{J}(k) = \frac{\partial|e(k)|^2}{\partial\mathbf{g}^*(k)} = 2e(k)\frac{\partial e(k)}{\partial\mathbf{g}^*(k)} \tag{24}$$

since

$$e(k) = \angle d(k) - \angle y(k) = \angle d(k) + \angle y^*(k) \tag{25}$$

and

$$y^*(k) = \mathbf{x}^H(k)\mathbf{h}^*(k) + \mathbf{x}^T(k)\mathbf{g}^*(k) \tag{26}$$

Hence

$$\frac{\partial e(k)}{\partial \mathbf{g}^*(k)} = \frac{\partial \angle y^*(k)}{\partial \mathbf{g}^*(k)} = \frac{\partial\left(\arctan\left(\frac{\Im(y^*(k+1))}{\Re(y^*(k+1))}\right) \pm \pi\right)}{\partial \mathbf{g}^*(k)}$$
$$= \frac{1}{1+\left(\frac{\Im(y^*(k))}{\Re(y^*(k))}\right)^2} \cdot \frac{\Re(y^*(k))\frac{\partial \Im(y^*(k))}{\partial \mathbf{g}^*(k)} - \Im(y^*(k))\frac{\partial \Re(y^*(k))}{\partial \mathbf{g}^*(k)}}{\Re^2(y^*(k))} \tag{27}$$

Using the following relations

$$\Re(y^*(k)) = \frac{(y^*(k) + y(k))}{2} \tag{28}$$

$$\Im(y^*(k)) = \frac{(y^*(k) - y(k))}{2\jmath} \tag{29}$$

and substituting (26) into (27), we obtain

$$\frac{\partial e(k)}{\partial \mathbf{g}^*(k)} = -\frac{\jmath \mathbf{x}(k)}{2(\mathbf{x}^T(k)\mathbf{h}(k) + \mathbf{x}^H(k)\mathbf{g}(k))^*} \tag{30}$$

Finally, the weight update for the conjugate filter coefficient $\mathbf{g}(k)$ becomes

$$\mathbf{g}(k+1) = \mathbf{g}(k) + \frac{\jmath\mu e(k)\mathbf{x}(k)}{(\mathbf{x}^T(k)\mathbf{h}(k) + \mathbf{x}^H(k)\mathbf{g}(k))^*} \tag{31}$$

In a similar way, the weight update of the coefficient vector $\mathbf{h}(k)$ can be obtained as

$$\mathbf{h}(k+1) = \mathbf{h}(k) - \mu\nabla_{\mathbf{h}}\mathcal{J}(k) = \mathbf{h}(k) - 2e(k)\frac{\partial e(k)}{\partial \mathbf{h}^*(k)}$$
$$= \mathbf{h}(k) + \frac{\jmath\mu e(k)\mathbf{x}^*(k)}{(\mathbf{x}^T(k)\mathbf{h}(k) + \mathbf{x}^H(k)\mathbf{g}(k))^*} \tag{32}$$

The expressions (31) and (32) describe the proposed widely linear LMP (WL-LMP) algorithm in the vector form, designed for phase angle error based adaptive estimation of the generality of complex signals.

For instantaneous frequency estimation in power systems, we need to use a scalar version of WL-LMP, given by

$$\hat{v}(k+1) = v(k)h(k) + v^*(k)g(k) \tag{33}$$

where from (31) and (32) the filter coefficient updates become

$$h(k+1) = h(k) + \frac{\jmath\mu e(k)v^*(k)}{(v(k)h(k) + v^*(k)g(k))^*}$$
$$g(k+1) = g(k) + \frac{\jmath\mu e(k)v(k)}{(v(k)h(k) + v^*(k)g(k))^*} \tag{34}$$

with $e(k) = \angle v(k+1) - \angle\hat{v}(k+1)$.

5.2. A WL-LMP based frequency estimator in power systems

Following on the analysis in [17], by substituting (9) into (33), the estimate of Clarke's voltage $\hat{v}(k+1)$ in (33) can be expressed as

$$\hat{v}(k+1) = Ah(k)e^{\jmath(\omega k\Delta T+\phi)} + Bh(k)e^{-\jmath(\omega k\Delta T+\phi)}$$
$$+ A^*g(k)e^{-\jmath(\omega k\Delta T+\phi)} + B^*g(k)e^{\jmath(\omega k\Delta T+\phi)}$$
$$= (Ah(k) + B^*g(k))e^{\jmath(\omega k\Delta T+\phi)} + (A^*g(k)$$
$$+ Bh(k))e^{-\jmath(\omega k\Delta T+\phi)} \tag{35}$$

while from (9) the expression for $v(k+1)$ can be re-written as

$$v(k+1) = Ae^{\jmath\omega\Delta T}e^{\jmath(\omega k\Delta T+\phi)} + Be^{-\jmath\omega\Delta T}e^{-\jmath(\omega k\Delta T+\phi)} \tag{36}$$

At the steady state, the first term on the right hand side (RHS) of (36) can be estimated approximately by its counterpart in (35), hence, the term $e^{\jmath\omega\Delta T}$ containing the frequency information is governed by

$$e^{\jmath\hat{\omega}\Delta T} = \frac{Ah(k) + B^*g(k)}{A} \tag{37}$$

Comparing the second terms on the RHS of (35) and (36), the evolution of $e^{-\jmath\omega\Delta T}$ can be expressed as

$$e^{-\jmath\hat{\omega}\Delta T} = \frac{A^*g(k) + Bh(k)}{B} \tag{38}$$

Upon applying the complex conjugation, we obtain

$$e^{\jmath\hat{\omega}\Delta T} = \frac{Ag^*(k) + B^*h^*(k)}{B^*} \tag{39}$$

which allows us to combine (37) and (39), to yield

$$e^{\jmath\hat{\omega}\Delta T} = h(k) + \frac{B^*}{A}g(k) \tag{40}$$

and

$$e^{\jmath\hat{\omega}\Delta T} = h^*(k) + \frac{A}{B^*}g^*(k) \tag{41}$$

As shown in (10), the coefficient A is real-valued whereas B is complex-valued, and thus $\frac{B^*}{A} = \left(\frac{B}{A}\right)^*$. Since (40) should be equal to (41), using $a(k) = \left(\frac{B}{A}\right)^*$ we can find $a(k)$ by solving the following quadratic equation with complex-valued coefficients

$$g(k)a^2(k) + (h(k) - h^*(k))a(k) - g^*(k) = 0 \tag{42}$$

The discriminant of this quadratic equation is given by

$$\Delta = \sqrt{(h(k) - h^*(k))^2 + 4|g(k)|^2} = 2\sqrt{-\Im^2(h(k)) + |g(k)|^2} \tag{43}$$

Since $a(k)$ is complex-valued, the discriminant is negative, and the two roots can be found from

$$a_1(k) = \frac{-\jmath\Im(h(k)) + \jmath\sqrt{\Im^2(h(k)) - |g(k)|^2}}{g(k)}$$
$$a_2(k) = \frac{-\jmath\Im(h(k)) - \jmath\sqrt{\Im^2(h(k)) - |g(k)|^2}}{g(k)} \tag{44}$$

while based on (40), the phasor $e^{\jmath\hat{\omega}\Delta T}$ is estimated either by using $h(k) + a_1(k)g(k)$ or $h(k) + a_2(k)g(k)$. Since the system frequency is far smaller than the sampling frequency, the imaginary part of $e^{\jmath\hat{\omega}\Delta T}$ is positive, thus excluding the second solution based on $a_2(k)$. The system frequency $\hat{f}(k)$ is therefore estimated in the form

$$\hat{f}(k) = \frac{1}{2\pi\Delta T}\tan^{-1}\left(\frac{\Im(h(k) + a_1(k)g(k))}{\Re(h(k) + a_1(k)g(k))}\right) \tag{45}$$

The above equation represents a generic widely linear extension of the standard, strictly linear, frequency estimation method and simplifies into the strictly linear LMP frequency estimator, given in (16), when the system is balanced ($g(k) = 0$).

5.3. Geometric interpretation

Fig. 1 provides a geometric interpretation of the frequency estimation procedure employed by the proposed WL-LMP algorithm. In unbalanced system conditions, where $B \neq 0$, the system voltage $v(k)$ comprises of two components, as shown in (9). The first term $A(k)$ rotates anticlockwise at the rate of the angular system frequency ω, whereas the second term $B(k)$, rotates clockwise at the same rate. The original LMP algorithm uses (12) and (13) to track the phase angle difference ϕ_L between $v(k)$ and $v(k+1)$, resulting in unavoidable estimation oscillations, as shown in (19). The

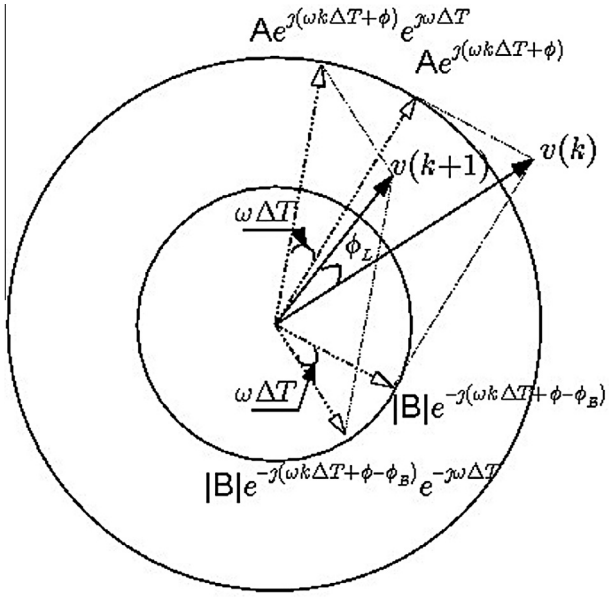

Fig. 1. Geometric illustration of the phase angle tracking of the noncircular complex-valued system voltage $v(k)$ by the strictly linear LMP and the proposed WL-LMP. The phasor $A(k)$ rotates counterclockwise, whereas the phasor $B(k)$ rotates clockwise.

proposed WL-LMP algorithm solves this problem by using (37) and (39) to track the phase differences between $A(k)$ and $A(k+1)$ and between $B(k)$ and $B(k+1)$, both containing the information about the exact angular system frequency ω, and leading to an unbiased and minimum variance frequency estimator, proposed in (45), for both balanced and unbalanced power systems.

6. Stability analysis of the WL-LMP frequency estimator

We next provide convergence and stability analysis of the proposed WL-LMP frequency estimator. Notice that for the LMP class of filters, the filter output is also contained in the denominator of the weight update, as shown in (14) and (34), so that the LMP has an inherent feedback. The stability bound for the step-size is then obtained following the approaches in [26,27]. To this end, the weight updates of the proposed algorithm, given in (31) and (32), are first written in a more compact form as

$$\mathbf{w}^a(k+1)=\mathbf{w}^a(k)+\frac{\jmath\mu e(k)\mathbf{v}^{a*}(k)}{(\mathbf{v}^{aT}(k)\mathbf{w}^a(k))^*} \tag{46}$$

where $\mathbf{w}^a(k)=[h(k),\,g(k)]^T$ and $\mathbf{v}^a(k)=[v(k),\,v^*(k)]^T$ are respectively the augmented weight and input vectors. We next consider the *a priori* and the *a posteriori* estimation errors, given respectively by

$$\hat{e}(k)=\angle v(k+1)-\angle\mathbf{v}^{aT}(k)\mathbf{w}^a(k) \tag{47}$$

$$\bar{e}(k)=\angle v(k+1)-\angle\mathbf{v}^{aT}(k)\mathbf{w}^a(k+1) \tag{48}$$

To estimate the range of μ which ensures that $|\bar{e}(k)|^2<|\hat{e}(k)|^2$ in the sense of mean square convergence, consider the first order Taylor series expansion (TSE) of $|\bar{e}(k)|^2$ around $|\hat{e}(k)|^2$, given by Ref. [28,26]

$$|\bar{e}(k)|^2=|\hat{e}(k)|^2+\Delta\mathbf{w}^{aH}(k)\frac{\partial|\hat{e}(k)|^2}{\partial\mathbf{w}^{a*}(k)} \tag{49}$$

where

$$\Delta\mathbf{w}^a(k)=\mathbf{w}^a(k+1)-\mathbf{w}^a(k)=\frac{\jmath\mu\hat{e}(k)\mathbf{v}^{a*}(k)}{(\mathbf{v}^{aT}(k)\mathbf{w}^a(k))^*} \tag{50}$$

and the gradient term

$$\frac{\partial|\hat{e}(k)|^2}{\partial\mathbf{w}^{a*}(k)}=\frac{-\jmath\hat{e}(k)\mathbf{v}^{a*}(k)}{(\mathbf{v}^{aT}(k)\mathbf{w}^a(k))^*} \tag{51}$$

In this way, the TSE in (49) can be rewritten as

$$\begin{aligned}|\bar{e}(k)|^2&=|\hat{e}(k)|^2-\frac{\mu|\hat{e}(k)|^2\|\mathbf{v}^a(k)\|_2^2}{|\mathbf{v}^{aT}(k)\mathbf{w}^a(k)|^2}\\&=\left(1-\frac{\mu\|\mathbf{v}^a(k)\|_2^2}{|\mathbf{v}^{aT}(k)\mathbf{w}^a(k)|^2}\right)|\hat{e}(k)|^2\end{aligned} \tag{52}$$

To guarantee $|\bar{e}(k)|^2<|\hat{e}(k)|^2$, and thus a stable filtering operation, we need to ensure that

$$|\bar{e}(k)|^2=\left(1-\frac{\mu\|\mathbf{v}^a(k)\|_2^2}{|\mathbf{v}^{aT}(k)\mathbf{w}^a(k)|^2}\right)^k|\hat{e}(0)|^2\overset{k\to\infty}{\longrightarrow}0 \tag{53}$$

that is, during the weight evolution we must ensure that

$$\left|1-\frac{\mu\|\mathbf{v}^a(k)\|_2^2}{|\mathbf{v}^{aT}(k)\mathbf{w}^a(k)|^2}\right|<1 \tag{54}$$

thus giving the stability bound on the step-size in the form

$$0<\mu<\frac{2|\mathbf{v}^{aT}(k)\mathbf{w}^a(k)|^2}{\|\mathbf{v}^a(k)\|_2^2} \tag{55}$$

7. Simulations

In the simulations, we considered frequency estimation under several unbalanced operating conditions (voltage sags), typically encountered by real world power systems. A voltage sag is referred to as a short-duration (up to a few seconds) reduction in voltage magnitude, whereby the the three phase-angles also deviate from their nominal positions. Voltage sags are mainly triggered by a short-term increase in load current, and may occur due to motor starting, transformer inrush, short circuits, or fast reclosing of circuit breakers [29]. Despite their short duration, such events can cause serious problems for a wide range of equipment [30] and also cause difficulties in standard phase angle calculation, resulting in oscillatory estimation artifacts at twice the system frequency, experienced by conventional PLL and strictly linear adaptive filters [16,17].

To quantify the characteristics of voltage sags, we here follow the phasor representation used in [29], and select two typical sags, known as Type C and Type D sags, for illustration purpose. A Type C sag results from a phase-to-phase fault, causing two phase voltages to move towards each other whereas the third phase voltage remains unchanged. Assuming that the fault occurs between the phases v_b and v_c, we have

$$\mathrm{V}_a=1,\quad \mathrm{V}_b=-\frac{1}{2}-\frac{\jmath\sqrt{3}\gamma}{2},\quad \text{and } \mathrm{V}_c=-\frac{1}{2}+\frac{\jmath\sqrt{3}\gamma}{2} \tag{56}$$

whereas in a Type D voltage sag all the three phases experience a voltage drop in the following way

$$\mathrm{V}_a=\gamma,\quad \mathrm{V}_b=-\frac{\gamma}{2}-\frac{\jmath\sqrt{3}}{2},\quad \text{and } \mathrm{V}_c=-\frac{\gamma}{2}+\frac{\jmath\sqrt{3}}{2} \tag{57}$$

For more information on the characterisation of voltage sags and their detection, we refer to [31,32].

Fig. 2 illustrates the circularity properties corresponding to various system imbalances. To illustrate the suitability of the proposed WL-LMP frequency estimator for unbalanced system conditions, a comparative performance analysis was conducted against the original LMP and the conventional mean square error based WL-CLMS algorithm [33]. Simulations in the Matlab programming environment employed a sampling frequency of

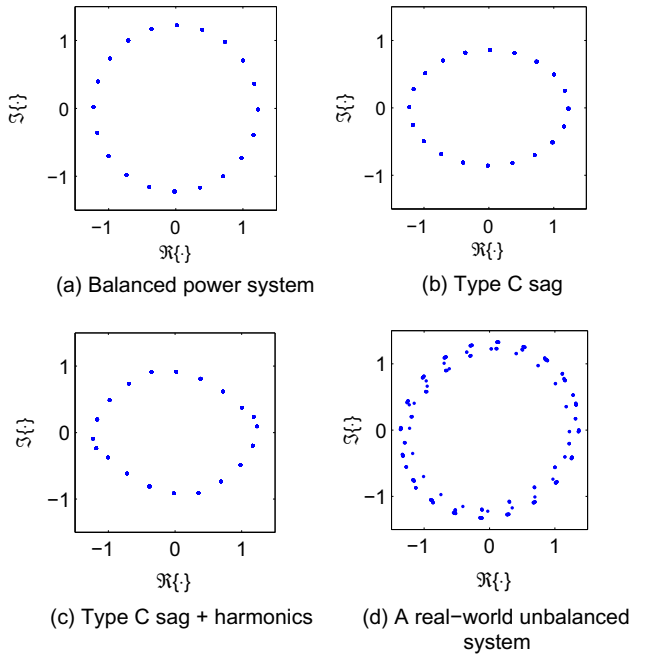

Fig. 2. Geometric view of the noncircularity of the complex-valued system voltage $v(k)$ via 'real-imaginary' scatter plots. The complex-valued voltage $v(k)$ rotates anticlockwise as the time evolves.

1000 Hz with the nominal fundamental power system frequency set to $f = 50$ Hz[1]. The step-size was kept at $\mu = 0.01$ for all the algorithms considered and the characteristic voltage γ was set to be 0.7 for the voltage sag modelling. The degree of noncircularity in different unbalanced conditions was quantified using the noncircularity index η, given by Ref. [22]

$$\eta = \frac{|\rho_v^2|}{\sigma_v^2} \tag{58}$$

Thus, the values of the noncircularity index η lie in the interval [0, 1], with the value 0 indicating that the complex-valued system voltage $v(k)$ is perfectly circular (balanced conditions), otherwise indicating a second-order noncircular $v(k)$ (unbalanced conditions).

7.1. Synthetic benchmark cases

In the first set of simulations, the simulated unbalanced power system experienced a Type C voltage sag. The noncircularity index of the complex-valued system voltage $v(k)$ obtained by the $\alpha\beta$ transformation of the three-phase voltage was $\eta = 0.3423$, and its noncircular distribution is illustrated by the geometric view of the distribution given in Fig. 2(b). The frequency estimation using all the algorithms, whose frequency carrying parameter was initialised at 50.1 Hz, is illustrated in Fig. 3. The strictly linear LMP frequency estimator experienced unavoidable oscillation error at twice the system frequency, which conforms with the analysis in (19), due to a breakdown of the strictly linear model employed in the phase angle calculation. Both the WL-LMP and WL-CLMS algorithms were able to eliminate this problem, leading to unbiased estimation and faster tracking performance achieved by the WL-LMP over WL-CLMS, a result of the superiority of phase angle error based cost function in the context of frequency estimation.

[1] We have observed that for both LMP and the proposed WL-LMP frequency estimators, the minimum sampling frequency should be about 4 times the system frequency we wish to track, and that there is no upper bound on the sampling frequency.

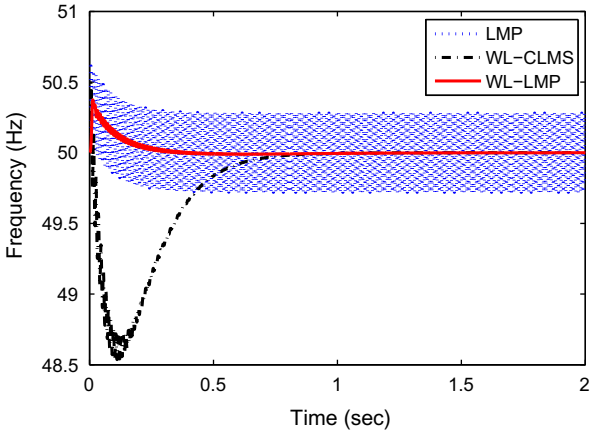

Fig. 3. Frequency estimation under the unbalanced Type C voltage sag. For all the algorithms, the initial frequency $f(0)$ was set to 50.1 Hz, with the true system frequency at 50 Hz.

It is well known in the adaptive filtering literature that the step size μ controls the tradeoff between the convergence speed and estimation accuracy in the steady state; in this way a smaller step size μ leads to better steady state performance and slower convergence, whereas a larger step-size results in faster convergence but larger steady-state estimation error [34]. As shown in Fig. 3, with $\mu = 0.01$, the proposed WL-LMP algorithm needs around 0.5 s, equivalently 500 samples (0.5 s $\times$ 1 kHz), to converge. In order to speed up the convergence and hence to ensure that fewer samples are required, a larger step-size μ can be used at a cost of higher estimation variance. However, we should note that the upper bound on the step-size μ to ensure the stability of the proposed WL-LMP is bounded by Eq. (55).

In the next stage, statistical performances of all the considered algorithms were tested in noisy environments, providing bias and variance analysis of the LMP frequency estimates. Fig. 4 illustrates the statistical bias and variance performance of all the considered algorithms, when applied to frequency estimation under the unbalanced Type C sag and against different levels of noise. The result was obtained by averaging 100 independent trails. Observe that both the bias and estimation variance of the strictly linear LMP algorithm were high and were not sensitive to the level of noise. This can be explained by the fact that, compared with noise contribution to the estimation error, the unavoidable bias and oscillation resulting from the inadequacy of strictly linear models, were dominant. The asymptotically unbiased nature of the widely linear model based WL-CLMS and WL-LMP can be observed in the high SNR region in Fig. 4(a), where the enhanced immunity to noise of the proposed WL-LMP as compared with the WL-ACLMS can also be observed. In Fig. 4(b), an improvement of around 2.5 dB in the estimation variance was achieved for different levels of noise by employing the phase error based cost function to train the widely linear adaptive filter.

Next, the performances of the widely linear frequency estimators under a more dynamically complex Type C voltage sag was addressed, whereby the unbalanced system experienced a slow amplitude modulation at 1 Hz, given by $V_a(k) = 1 + 0.15$ sin $(2\pi k\Delta T)$, $V_b(k) = 1 + 0.1$ sin $(2\pi k\Delta T)$, and $V_c(k) = 1 + 0.1$ sin $(2\pi k\Delta T)$, resulting in a noncircular complex-valued system voltage $v(k)$ with a degree of noncircularity $\eta = 0.3444$. Fig. 5 shows that due to the breakdown of the implicit assumption that exists in standard frequency estimation methods, that is, the magnitude of the complex-valued system voltage $v(k)$ is time-invariant, both WL-CLMS and WL-LMP were subject to an oscillatory estimation error. However, the proposed WL-LMP tracked the true system

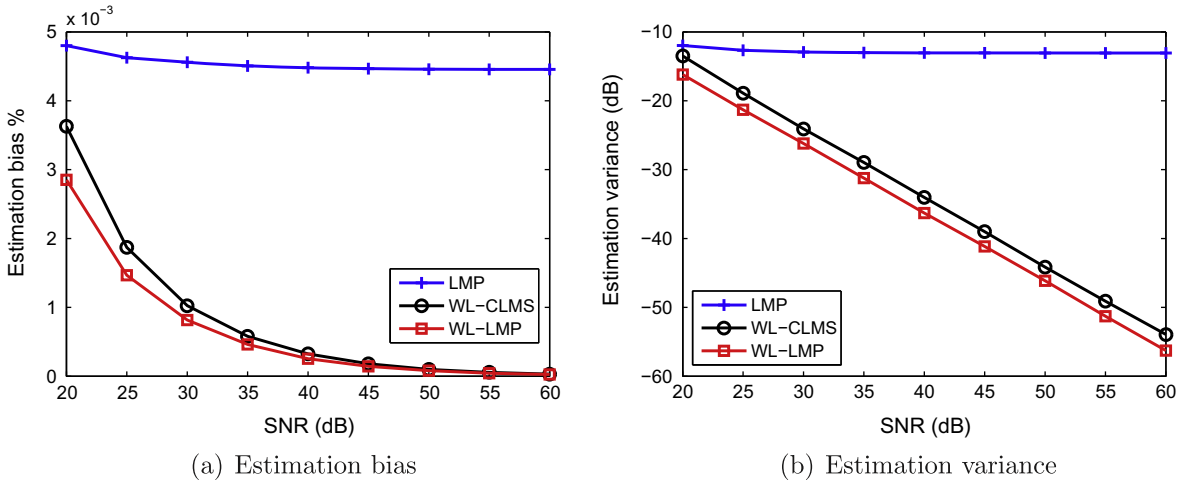

(a) Estimation bias (b) Estimation variance

Fig. 4. Bias and variance analysis of all the frequency estimators considered, at different SNRs from 20 to 50 dB, obtained by averaging 100 independent trials.

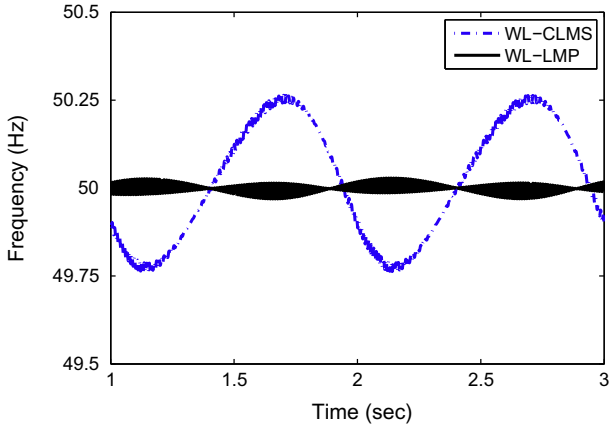

Fig. 5. Impact of oscillatory variations of amplitude on the frequency estimation by WL-CLMS and WL-LMP.

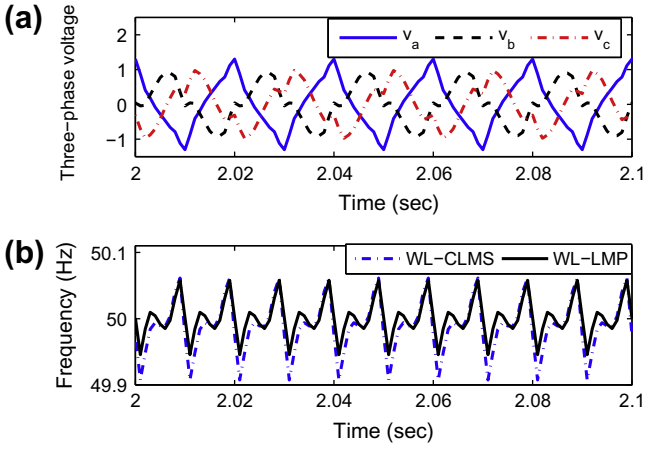

Fig. 6. Frequency estimation by WL-CLMS and WL-LMP under Type C unbalanced voltage sag and in the presence of higher order harmonics. (a) The waveforms of the three-phase voltage, which were distorted by 20% 3rd, 10% 5th, and 5% 7th harmonics. (b) Estimation performance.

frequency more accurately exhibiting a maximum 0.03 Hz estimation deviation as compared with 0.25 Hz estimation deviation experienced by the WL-CLMS.

To examine robustness to contamination by higher order harmonics, the unbalanced system under Type C voltage sag was next polluted by 20% 3rd, 10% 5th, and 5% 7th harmonics of the fundamental frequency. The voltage waveforms of this highly distorted three-phase voltage are shown in Fig. 6(a), giving a noncircular system voltage $v(k)$, whose distribution is given in Fig. 2(c), with $\eta = 0.342$. The proposed WL-LMP achieved better performance and with smaller error oscillation as compared with the magnitude-phase WL-CLMS algorithm, as shown in Fig. 6(b).

Finally, the performances of all the algorithms were compared for the cases of frequency decay and rise when an unbalanced power system experienced a Type D voltage sag. In Fig. 7(a), the 50 Hz fundamental frequency of the system arose and decayed at a rate of 2 Hz/s. The LMP was biased and with large estimation variance, whereas the proposed WL-LMP showed very fast frequency tracking ability as compared with WL-CLMS, and its superior estimation accuracy over WL-CLMS is illustrated in Fig. 7(b).

7.2. Real world case study

In the last set of simulations, we considered a real-world problem, where unbalanced three-phase voltages were recorded at a 110/20/10 kV transformer station. The REL 531 numerical line distant protection terminal, produced by ABB Ltd., was installed in the station and was used to monitor changes in the three phase ground voltages. The measured three phase-ground voltages with a system frequency of 50 Hz were sampled at 1 kHz and were normalised with respect to their normal peak voltage values. Two case studies were conducted. In the first case, as shown in Fig. 8(a), initially, the three phases were in their normal and balanced condition, lasting for around 0.03 s, and all three algorithms tracked the system frequency during this period in a similar manner. However, after 0.03 s, phase v_b experienced an earth fault, causing a 66.8% voltage drop and 73.7% and 55.2% voltage swells in phases v_a and v_c respectively. This gave the $\alpha\beta$ transformed system voltage the degree of noncircularity of $\eta = 0.109$, with a noncircularity diagram shown in Fig. 2(d). In the second case study, a more critically unbalanced condition was investigated. As shown in Fig. 9(a), at around 0.05 s, both phases v_a and v_c experienced 137.1% and 122.8% voltage swells, respectively, whereas phase v_b experienced a 85.5% voltage drop, giving the system voltage a degree of noncircularity of $\eta = 0.241$. As shown in both Fig. 8(b) and Fig. 9(b), the strictly linear LMP suffered large frequency estimation oscillations under the unbalanced conditions, whereas the proposed WL-LMP outperformed the WL-CLMS exhibiting both a smoother transient and a smaller estimation variance in the steady state.

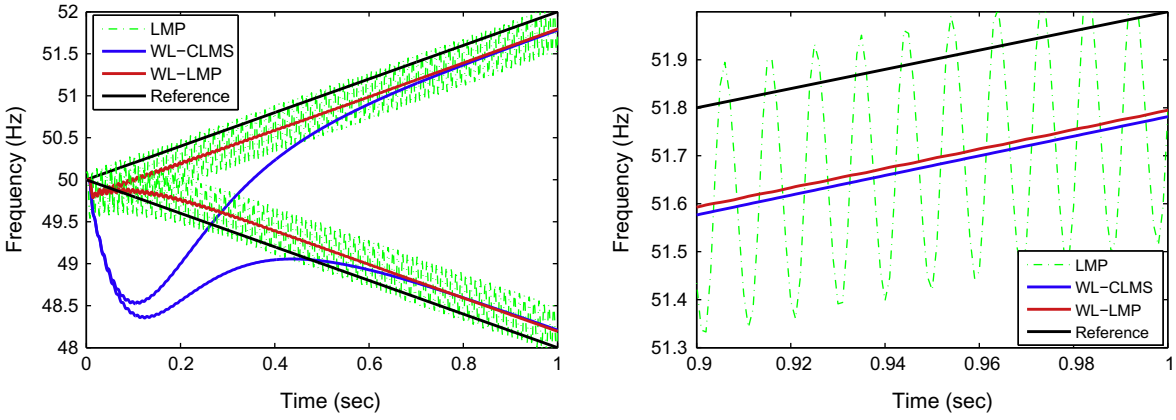

(a) Estimation over a 1 sec segment (b) A zoom into the last 0.1 sec

Fig. 7. Frequency estimation of all the algorithms for an unbalanced power system under a Type D voltage sag, with system frequency undergoing the decay and rise respectively at a rate of 2 Hz/s.

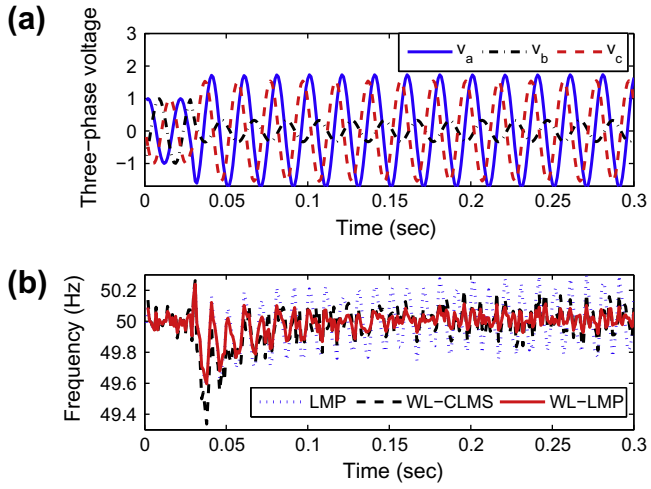

Fig. 8. Frequency estimation by all the algorithms for real-world unbalanced three-phase voltages (Case study 1). (a) The waveforms of the three-phase voltage. (b) Frequency estimation of all algorithms considered.

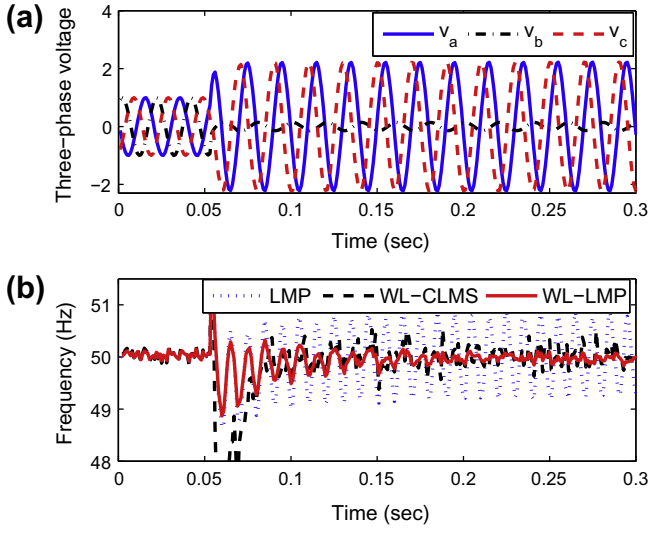

Fig. 9. Frequency estimation by all the algorithms for real-world unbalanced three-phase voltages (Case study 2). (a) The waveforms of the three-phase voltage. (b) Frequency estimation of all algorithms considered.

8. Conclusion

We have introduced a robust widely linear least mean phase (WL-LMP) technique for real-time estimation of the fundamental frequency in unbalanced and distorted power systems. This has been achieved by combining a phase error based cost function with the widely linear estimation model. We have shown that the conjugate part within the widely linear model corrects the phase angle calculation error exhibited by the strictly linear model, which suffers from unavoidable estimation bias and oscillation issues under unbalanced system conditions. The proposed unbiased frequency estimator, based on WL-LMP, has been shown to outperform the error power based WL-CLMS frequency estimator. Simulations over a range of unbalanced conditions, including voltage sags, the presence of higher order harmonics, and for real-world case studies support the analysis.

Acknowledgement

The authors thank Mr. Z. Blazic of Elektroprenos, BiH, for providing real-world data, fruitful discussions, and expert advice.

References

[1] Sachdev MS, Giray MM. A least error squares technique for determining power system frequency. IEEE Trans Power Appar Syst – PAS 1995;104(2):437–44.
[2] Dugan RC, McGranaghan MF, Santoso S, Beaty HW. Electrical power systems quality. McGraw-Hill; 2002.
[3] Begovic MM, Djuric PM, Dunlap S, Phadke AG. Frequency tracking in power networks in the presence of harmonics. IEEE Trans Power Del 1993;8(2):480–6.
[4] Hancke GP. The optimal frequency estimation of a noisy sinusoidal signal. IEEE Trans Instrum Meas 1990;39(6):843–6.
[5] Phadke AG, Thorp J, Adamiak M. A new measurement technique for tracking voltage phasors, local system frequency and rate of change of frequency. IEEE Trans Power Appl Syst – PAS 1983;102(5):1025–38.
[6] Yang J, Liu C. A precise calculation of power system frequency and phasor. IEEE Trans Power Del 2000;15(2):494–9.
[7] Karimi H, Karimi-Ghartemani M, Iravani MR. Estimation of frequency and its rate of change for applications in power systems. IEEE Trans Power Del 2004;19(2):472–80.
[8] Indu Rani B, Aravind CK, Saravana Iiango G, Nagamini C. A three phase PLL with a dynamic feedforward frequency estimator for synchronization of grid connected converters under wide frequency variations. Int J Electr Power Energy Syst 2012;41(1):63–70.
[9] Pradhan AK, Routray A, Basak A. Power system frequency estimation using least mean square technique. IEEE Trans Power Del 2005;20(3):761–6.
[10] Barbosa D, Monaro RM, Coury DV, Oleskovicz M. Digital frequency relaying based on the modified least mean square method. Int J Electr Power Energy Syst 2010;32(3):236–42.

[11] Terzija V, Djuric M. Direct estimation of voltage phasor, frequency and its rate of change using Newton's iterative method. Int J Electr Power Energy Syst 1994;16(6):423–8.
[12] Dash PK, Jena RK, Panda G, Routray A. An extended complex Kalman filter for frequency measurement of distorted signals. IEEE Trans Instrum Meas 2000;49(4):746–53.
[13] Routray A, Pradhan AK, Rao KP. A novel Kalman filter for frequency estimation of distorted signals in power systems. IEEE Trans Instrum Meas 2002;51(3):469–79.
[14] Tarighat A, Sayed AH. Least mean-phase adaptive filters with application to communications systems. IEEE Signal Process Lett 2004;11(2):220–3.
[15] Rawat TK, Parthasarathy H. A continuous-time least mean-phase adaptive filter for power frequency estimation. Int J Electr Power Energy Syst 2009;31:111–5.
[16] Song H, Nam K. Instantaneous phase-angle estimation algorithm under unbalanced voltage-sag conditions. Proc Inst Elect Eng 2000;147(6):409–15.
[17] Xia Y, Mandic DP. Widely linear adaptive frequency estimation of unbalanced three-phase power system. IEEE Trans Instrum Meas 2012;61(1):74–83.
[18] Xia Y, Douglas SC, Mandic DP. Adaptive frequency estimation in smart grid applications: exploiting noncircularity and widely linear adaptive estimators. IEEE Signal Process Mag 2012;29(5):44–54.
[19] Xia Y, Mandic DP. Augmented MVDR spectrum-based frequency estimation for unbalanced power systems. IEEE Trans Instrum Meas 2013;62(7):1917–26.
[20] Neeser FD, Massey JL. Proper complex random processes with applications to information theory. IEEE Trans Inform Theory 1993;39(4):1293–302.
[21] Picinbono B, Chevalier P. Widely linear estimation with complex data. IEEE Trans Signal Process 1995;43(8):2030–3.
[22] Mandic DP, Goh SL. Complex valued nonlinear adaptive filters: noncircularity. Widely linear and neural models. John Wiley & Sons; 2009.
[23] Xia Y, Jelfs B, Hulle MMV, Príncipe JC, Mandic DP. An augmented echo state network for nonlinear adaptive filtering of complex noncircular signals. IEEE Trans Neural Netw 2011;22(1):74–83.
[24] Clarke E. Circuit analysis of AC power systems. New York: Wiley; 1943.
[25] Akke M. Frequency estimation by demodulation of two complex signals. IEEE Trans Power Del 1997;12(1):157–63.
[26] Mandic DP, Chambers JA. Recurrent neural networks for prediction: learning algorithms. Architectures and stability. John Wiley & Sons; 2001.
[27] Cheong Took C, Mandic DP. Adaptive IIR filtering of noncircular complex signals. IEEE Trans Signal Process 2009;57(10):4111–8.
[28] Soria-Olivas E, Calpe-Maravilla J, Guerrero-Marinez JF, Martinez-Sober M, Espi-Lopez J. An easy demonstration of the optimum value of the adaptation constant in the LMS algorithm [FIR filter theory]. IEEE Trans Educat 1998;41(1):81.
[29] Bollen MHJ. Characterisation of voltage sags experienced by three-phase adjustable-speed drives. IEEE Trans Power Del 1997;12(4):1666–71.
[30] Honrubia-Escribano A, Gómez-Lázaro E, Molina-García A, Fuentes JA. Influence of voltage dips on industrial equipment: analysis and assessment. Int J Electr Power Energy Syst 2012;41:87–95.
[31] Tavakoli Bina M, Kashefi A. Three-phase unbalance of distribution systems: complementary analysis and experimental case study. Int J Electr Power Energy Syst 2011;33:817–26.
[32] Chen T-H, Yang C-H, Yang N-C. Examination of the definitions of voltage unbalance. Int J Electr Power Energy Syst 2013;49:380–5.
[33] Javidi S, Pedzisz M, Goh SL, Mandic DP. The augmented complex least mean square algorithm with application to adaptive prediction problem. In: Proc 1st IAPR workshop cogn inf process; 2008. p. 54–7.
[34] Sayed AH. Fundamentals of adaptive filtering. New York: Wiley; 2003.